SIMULATION OF STATISTICAL MEAN BEHAVIORS AND COHERENT STRUCTURES OF INCOMPRESSIBLE TURBULENT FLOWS USING UNILATERAL-AVERAGE BASED GOVERNING EQUATIONS

G.Gao. Beijing University of Aeronautics and Astronautics, Beijing 100083, CHINA
Y.Yong. Department of Ocean Engineering, Florida Atlantic University, FL 33431, USA

Abstract

This paper presents a preliminary study of incompressible turbulent flow using a unilateral statistical average scheme. As the ensemble average is taken on two groups of turbulence fluctuations separately, this average scheme is able to capture the first-order statistical information of the fluctuation field. Continuity, momentum, and mechanical energy equations are derived for the fluctuation field based on this valuable information. Concepts of orthotropic turbulence and momentum transfer chain are used to model correlation terms, and eventually lead to a complete set of equations of incompressible turbulence. These equations preserve the nonlinearity of typical turbulence and contain no empirical coefficients and wall functions. The mechanical energy equation, derived in the form of a series to reflect the typical multi-scale nonlinear phenomena, is able to describe statistical mean flow and coherent flow. Four benchmark turbulent flows, namely, plan jet, round jet, flat plate flow with laminar-turbulent transition, and backward facing step flow, are simulated for both statistical mean flows and coherent structures to verify the adaptability of the rationally derived equations.

The two authors have made equal contribution to this work.

1 Introduction

The study of turbulence has two major movements: statistics and structure. Both movements have their own perplexing questions. The coherent structures need primary theoretical explanation. The statistical models, on the other hand, have to face the closure problem, which is introduced by the conventional Reynolds average, and must rely on empiricism to introduce extra equations and empirical coefficients. Since there are no universal coefficients in any existing model to encounter the variety of flow cases, the closure problem has never been flawlessly solved.

It is the authors' belief that rational equations of turbulence can be obtained within the framework of Navier-Stokes equations and the main reason that turbulence remains unsolved for more than a century is lack of direct first-order statistical information of turbulence fluctuations. The conventional Reynolds average scheme does not recognize this information, leaving researchers with no other choices than relying on higher order statistics. The present approach introduces a unilateral average scheme for the purpose of effectively extracting this information. In this approach, turbulent fluctuations are divided into two groups based upon a set criterion. The obtained nonzero symmetric ensemble averages of individual group of fluctuations are used to

define the momentum transfer chain and orthotropic turbulence. The former describes the momentum transfer from the mean flow to fluctuation flow, and then from fluctuation flow to molecular motions. The latter reflects the physics that turbulent fluctuations constitute non-isotropic viscosity for the mean flow. Both concepts direct the modeling of the correlation terms arising from the unilateral average and give rise to additional equations for the closure problem. As the number of unknowns is equal to the number of derived equations, no any empirical coefficients or wall functions are needed in this approach. Four benchmark flows, i.e., boundary layer flow (flat plate) and transition, free shear flow (plan/round jet), and separated flow (backward facing step) were simulated to verify the adaptability of the newly developed equations of turbulence. The same set of equations used in all flow conditions has produced promising results regarding laminar-turbulent transition, plan/round jet anomaly, and separation flow reattachment. Meanwhile, using the same set of equations also simulates the coherent flow structures of the four-benchmark flows.

2 Unilateral average scheme

In spite of its complexity, turbulent flow, in the minimum scale in which the concept of continuum mechanics is still valid, satisfies the Navier-Stokes equations. In the case of a large Reynold's number, the strong nonlinearity of N-S equations usually leads to an infinite number of solutions for a set of given initial conditions. Let u_i be one of the random samples in the solution space. The corresponding fluctuating velocity is defined as

$$u_i' = u_i - \overline{u} \qquad (1)$$

As a note, u, with or without sub-indexes, always denotes a velocity vector in the present analysis. The mean velocity in the above equation is obtained from the following ensemble average

$$\overline{u} = \lim_{N \to \infty} \frac{1}{N} \sum_{i=1}^{N} u_i \qquad (2)$$

in which N is the number of possible solutions of Navier-Stokes equations. Now, we divide the solutions into two groups according to a certain criterion. The fluctuation components in the two groups are denoted by u_i^{I} and u_i^{II}. The ensemble average of the fluctuations of the first group

$$\overline{u}^{I} = \lim_{N_I \to \infty} \frac{1}{N_I} \sum_{i=1}^{N_I} u_i^{I} \qquad (3)$$

is called the first drift velocity, where N_I is the number of solutions in the first group. Likewise, if N_{II} is the number of solutions in the second group, the second drift velocity is defined as

$$\overline{u}^{II} = \lim_{N_{II} \to \infty} \frac{1}{N_{II}} \sum_{i=1}^{N_{II}} u_i^{II} \qquad (4)$$

As the ensemble average of all fluctuations

$$\lim_{N,N_I \to \infty} \frac{\sum_{i=1}^{N_I} u_i^{I}}{N} + \lim_{N,N_{II} \to \infty} \frac{\sum_{i=1}^{N_{II}} u_i^{II}}{N} = \lim_{N,N_I \to \infty} \frac{N_I}{N} \frac{\sum_{i=1}^{N_I} u_i^{I}}{N_I} + \lim_{N,N_{II} \to \infty} \frac{N_{II}}{N} \qquad (5)$$

is zero,

$$M_I \overline{u}^{I} + M_{II} \overline{u}^{II} = 0 \qquad (6)$$

in which $M_I = N_I / N$ and $M_{II} = N_{II} / N$, and

$$M_I + M_{II} = 1 \qquad (7)$$

M_I and M_{II} are slowly varying weighting functions of x and t. The weighted average $\widetilde{u}^{I} = M_I \overline{u}^{I}$ and $\widetilde{u}^{II} = M_{II} \overline{u}^{II}$, satisfy:

$$\widetilde{u}^{I} + \widetilde{u}^{II} = 0 \qquad (8)$$

As the weighted drift velocities are symmetric, the information of the fluctuation field can be effectively represented by $\widetilde{u}^{I}$ alone. For convenience, the weighted drift flows are called drift flows in short. As the mean value of

pressure fluctuations p_i' vanishes throughout the turbulent flow, the weighted pressures $\tilde{p}^I$ and $\tilde{p}^{II}$ are also symmetric, i.e.

$$\tilde{p}^I + \tilde{p}^{II} = 0 \qquad (9)$$

3 Momentum Equations of drift flow

We now write the N-S equation for the i-th solution u_i as

$$\frac{\partial u_i}{\partial t} + (u_i \cdot \nabla) u_i = -\frac{1}{\rho} \nabla p_i + \frac{1}{\rho} \mu_L \nabla^2 u_i \qquad (10)$$

The ensemble average of (10) for all the solutions is

$$\frac{\partial \bar{u}}{\partial t} + (\bar{u} \cdot \nabla) \bar{u}$$
$$= -\frac{1}{\rho} \nabla \bar{p} + \frac{1}{\rho} \mu_L \nabla^2 \bar{u} - \overline{(u' \cdot \nabla) u'} \qquad (11)$$

where

$$\overline{(u' \cdot \nabla) u'} = \lim_{N \to \infty} \frac{1}{N} \sum_{i=1}^{N} (u_i' \cdot \nabla) u_i' \qquad (12)$$

Subtracting (11) from (10), we obtain the momentum equation for the i-th fluctuation

$$\frac{\partial u_i'}{\partial t} + (\bar{u} \cdot \nabla) u_i' + (u_i' \cdot \nabla) \bar{u} + (u_i' \cdot \nabla) u_i'$$
$$= -\frac{1}{\rho} \nabla p_i' + \frac{1}{\rho} \mu_L \nabla^2 u_i' + \overline{(u' \cdot \nabla) u'} \qquad (13)$$

The weighted ensemble average of (13) for the fluctuations of the first group is

$$\frac{\partial \tilde{u}^I}{\partial t} + (\bar{u} \cdot \nabla) \tilde{u}^I = -\frac{1}{\rho} \nabla \tilde{p}^I + \frac{1}{\rho} \mu_L \nabla^2 \tilde{u}^I$$
$$- (\tilde{u}^I \cdot \nabla) \bar{u} + M_I \overline{(u' \cdot \nabla) u'} - M_I \overline{(u^I \cdot \nabla) u^I} \qquad (14)$$

where

$$\overline{(u^I \cdot \nabla) u^I} = \lim_{N_I \to \infty} \frac{1}{N_I} \sum_{i=1}^{N_I} (u_i^I \cdot \nabla) u_i^I \qquad (15)$$

The weighted ensemble average of (13) for the fluctuations of the second group is likewise

$$\frac{\partial \tilde{u}^{II}}{\partial t} + (\bar{u} \cdot \nabla) \tilde{u}^{II} = -\frac{1}{\rho} \nabla \tilde{p}^{II} + \frac{1}{\rho} \mu_L \nabla^2 \tilde{u}^{II}$$
$$- (\tilde{u}^{II} \cdot \nabla) \bar{u} + M_{II} \overline{(u' \cdot \nabla) u'} - M_{II} \overline{(u^{II} \cdot \nabla) u^{II}} \qquad (16)$$

where

$$\overline{(u^{II} \cdot \nabla) u^{II}} = \lim_{N_{II} \to \infty} \frac{1}{N_{II}} \sum_{i=1}^{N_{II}} (u_i^{II} \cdot \nabla) u_i^{II} \qquad (17)$$

The condition for (14) and (16) to be valid is that M_1 and M_{II} are slowly varying functions of x and t. Such a condition should be met in the division of the fluctuation field. It can be proved that the three correlation terms given in (12), (15), and (17) are related as

$$\overline{(u' \cdot \nabla) u'} = M_I \overline{(u^I \cdot \nabla) u^I}$$
$$+ M_{II} \overline{(u^{II} \cdot \nabla) u^{II}} \qquad (18)$$

Substituting (18) into (14) and (16), respectively, we obtain

$$\frac{\partial \tilde{u}^I}{\partial t} + (\bar{u} \cdot \nabla) \tilde{u}^I = -\frac{1}{\rho} \nabla \tilde{p}^I + \frac{1}{\rho} \mu_L \nabla^2 \tilde{u}^I$$
$$- (\tilde{u}^I \cdot \nabla) \bar{u} - M_I M_{II} \left(\overline{(u^I \cdot \nabla) u^I} - \overline{(u^{II} \cdot \nabla) u^{II}} \right) \qquad (19)$$

$$\frac{\partial \tilde{u}^{II}}{\partial t} + (\bar{u} \cdot \nabla) \tilde{u}^{II} = -\frac{1}{\rho} \nabla \tilde{p}^{II} + \frac{1}{\rho} \mu_L \nabla^2 \tilde{u}^{II}$$
$$- (\tilde{u}^{II} \cdot \nabla) \bar{u} + M_I M_{II} \left(\overline{(u^I \cdot \nabla) u^I} - \overline{(u^{II} \cdot \nabla) u^{II}} \right) \qquad (20)$$

It is noted that the only difference between (19) and (20) is of the opposite signs of the last terms on the right of the equations.   It reconfirms that weighted drift flows $\tilde{u}^I$ and $\tilde{u}^{II}$ are symmetric.   Only one drift flow, say $\tilde{u}^I$, is, therefore, needed in the present analysis. Due to the symmetric property of two drift flows, we drop the superscript I and II in the following discussion for convenience.

4 Modeling

As usual, we model $\overline{(u' \cdot \nabla) u'}$ as the divergence of the turbulence stress tensor, i.e.

$$\overline{(u' \cdot \nabla) u'} = -\frac{1}{\rho} \nabla \cdot \overline{\tau}_T \qquad (21)$$

The momentum equation of the mean flow is, therefore, written as

$$\frac{\partial \overline{u}}{\partial t} + (\overline{u} \cdot \nabla) \overline{u} = -\frac{1}{\rho} \nabla \overline{p} +$$
$$\frac{1}{\rho} \mu_L \nabla^2 \overline{u} + \frac{1}{\rho} \nabla \cdot \overline{\tau}_T \qquad (22)$$

We now model

$$M_I M_{II} \overline{\left((u^I \cdot \nabla) u^I - \overline{(u^{II} \cdot \nabla) u^{II}}\right)}$$
$$= \frac{1}{\rho} \mu_L \nabla^2 \overline{u} + \frac{1}{\rho} \nabla \cdot \overline{\tau}_T - \frac{\nabla \cdot \widetilde{\tau}_T^I}{2\rho} + \frac{\nabla \cdot \widetilde{\tau}_T^{II}}{2\rho} \quad (23)$$

in which

$$\nabla \cdot \widetilde{\tau}_T^I = -\nabla \cdot \widetilde{\tau}_T^{II} \qquad (24)$$

It is important to note that any type of divisions of the fluctuation field will lead to the same set of equations (19) and (20). The division, however, becomes unique once the modeling equation (23) is introduced. Substituting (23) into (19) gives

$$\frac{\partial \widetilde{u}}{\partial t} + (\overline{u} \cdot \nabla) \widetilde{u} = -\frac{1}{\rho} \nabla \widetilde{p} + \frac{1}{\rho} \mu_L \nabla^2 (\widetilde{u} - \overline{u})$$
$$+ \frac{1}{\rho} \nabla \cdot (\widetilde{\tau}_T - \overline{\tau}_T) - (\widetilde{u} \cdot \nabla) \overline{u} \qquad (25)$$

The above equations clearly demonstrate a momentum transfer chain that begins from the mean flow. The momentum of the mean flow is first transferred to the drift flows through divergences of laminar and turbulence stresses of the mean flow. The next level of the momentum chain is the transfer of the momentum of the drift flows, again through divergences of stresses of the drift flow, to molecular motion in a form of heat.

5 Orthotropic constitutive relationship

To determine the turbulence stress tensor, we first observe the constitutive relationship between stresses and strains. For a non-isotropic turbulent flow, 36 constitutive coefficients are independent. These coefficients vary with the change of coordinate system. Because of the symmetry of the two weighted drift flows, it is reasonable to assess that the drift flow field constitutes an orthotropic environment for the mean flow. The orthotropic coordinate system may be set in the three principal material axes n_1, n_2, and n_3, where n_1 is in the mean streamline direction, and n_2 and n_3 are on the normal plane to the streamline. Due to the symmetry of the orthotropic coordinates, the coefficient matrix is greatly simplified, in which there are only 12 non-zero coefficients [1].

To model the orthotropic turbulence viscosity, we introduce the displacement vector λ of the drift flow field, and define eddy viscosity tensor as

$$\xi_{ij} = \lambda_j \widetilde{u}_i \qquad (26)$$

The constitutive equation with symmetric property is written as

$$\tau_{ij} = 2\mu_{IJ}\varepsilon_{ij} - \frac{2}{3}\mu_{KK}\varepsilon_{kk}\delta_{ij} \qquad (27)$$

where I, J, and K, taking the same values as i, j, and k, have no implication of summation, and

$$\mu_{IJ} = \left|\xi_{ij}\right| + \left|\xi_{ji}\right| \qquad (28)$$

Then, the strain-stress relationship in the xyz coordinates can be written as equation (29), in which [T] is a coordinate transformation matrix between the xyz and the principal material coordinate systems. It is obvious that the orthotropic coefficient matrix is quite simple due to the symmetry of drift flows, but there are still 36 nonzero non-isotropic viscosity coefficients after the coordinate transformation. The problem of anisotropy may be solved in this way.

$$
\begin{Bmatrix} \tau_{xx} \\ \tau_{yy} \\ \tau_{zz} \\ \tau_{xy} \\ \tau_{yz} \\ \tau_{zx} \end{Bmatrix} = 2[T]^{-1}
\begin{bmatrix}
\frac{4}{3}|\xi_{11}| & -\frac{2}{3}|\xi_{22}| & -\frac{2}{3}|\xi_{33}| & 0 & 0 & 0 \\
-\frac{2}{3}|\xi_{11}| & \frac{4}{3}|\xi_{22}| & -\frac{2}{3}|\xi_{33}| & 0 & 0 & 0 \\
-\frac{2}{3}|\xi_{11}| & -\frac{2}{3}|\xi_{22}| & \frac{4}{3}|\xi_{33}| & 0 & 0 & 0 \\
0 & 0 & 0 & |\xi_{12}|+|\xi_{21}| & 0 & 0 \\
0 & 0 & 0 & 0 & |\xi_{23}|+|\xi_{32}| & 0 \\
0 & 0 & 0 & 0 & 0 & |\xi_{31}|+|\xi_{13}|
\end{bmatrix}
[T]\begin{Bmatrix} \varepsilon_{xx} \\ \varepsilon_{yy} \\ \varepsilon_{zz} \\ \varepsilon_{xy} \\ \varepsilon_{yz} \\ \varepsilon_{zx} \end{Bmatrix} \quad (29)
$$

6 Mechanical energy equation

Vector λ is defined as the averaged value of the particle displacements of the first group's fluctuations. Its direction is assumed to coincide with the direction of the maximum tensile stress of the mean flow. Its magnitude can be determined from an independent mechanical energy equation that describes the relationship between the kinetic energy change of the mean flow due to the dragging effect of the drift flow and the work done by the drift flow. As the absolute velocity of drift flow in a fixed coordinate system is $\bar{u} + \tilde{u}$, the difference of kinetic energy of the drift flow at x and x+ λ can be expanded into the following Taylor's series

$$
\begin{aligned}
&\frac{1}{2}\left(\bar{u}(x+\lambda)+\tilde{u}(x+\lambda)\right)^2 - \frac{1}{2}\left(\bar{u}(x)+\tilde{u}(x)\right)^2 \\
&= \frac{1}{2}\sum_{n=1}^{\infty}\frac{(\lambda\cdot\nabla)^n\bar{u}^2}{n!} + \sum_{n=1}^{\infty}\frac{(\lambda\cdot\nabla)^n(\bar{u}\cdot\tilde{u})}{n!} \\
&\quad + \frac{1}{2}\sum_{n=1}^{\infty}\frac{(\lambda\cdot\nabla)^n\tilde{u}^2}{n!}
\end{aligned} \quad (30)
$$

The first term on the right hand side represents the mean flow kinetic energy change over displacement λ due to its own variation. Likewise, the third term represents the drift flow kinetic energy change over displacement λ due to its own variation. The second term represents the kinetic energy change due to the interaction of mean flow and drift flow, in which we are only interested in the following term：

$$
\sum_{n=1}^{\infty}\frac{1}{n!}(\lambda\cdot\nabla)^n\bar{u}\cdot\tilde{u}
$$

This term contains eddy viscosity tensor and mean velocity gradients, and stands for the mean flow kinetic energy change caused by the drag of drift flows. It is worthy to notice that the right hand side of the momentum equation of drift flow (25)，subtracting $D\bar{u}/Dt$, is the force applying to unit mass of the drift flow. The work done by this force over mean displacement λ should be equal to the change of kinetic energy of the mean flow due to the drag of the drift flow, i.e.

$$
\begin{aligned}
&\sum_{n=1}^{\infty}\frac{1}{n!}(\lambda\cdot\nabla)^n\bar{u}\cdot\tilde{u} = \lambda\cdot[-\frac{1}{\rho}\nabla\tilde{p} + \\
&\frac{1}{\rho}\nabla\cdot(\tilde{\tau}_L - \bar{\tau}_L) + \frac{1}{\rho}\nabla\cdot(\tilde{\tau}_T - \bar{\tau}_T) \\
&- (\tilde{u}\cdot\nabla)\bar{u} - \frac{D\bar{u}}{Dt}]
\end{aligned} \quad (31)
$$

The independent equation (31) signifies dynamic equilibrium of the mean flow kinetic energy change and work done by the drift flow. The series form on the left hand side of the above equation corresponds to numerous scales of turbulence coherent structures up to the n-th order. If n is infinity, we can obtain statistical mean flow in an absolute sense. But for engineering applications, n=1 usually leads to first-order coherent structure flow, n=2 gives approximate statistical mean solutions for

moderate turbulence and n=3 is suitable for ultra-strong turbulent mean flows. Therefore, it is seen that statistical mean flow and coherent flow are controlled by the same equation (31) but characterized by different order n in the equation. When calculating statistical mean flow, one may start with the first order energy equation. If coherent behaviors appear, higher order n should be used. In the numerical computation, we also need to use the coefficient of substance C_s to express the effect of flow dimensions and boundary wall on the eddy viscosity tensor such as

$$\xi = C_s \lambda \widetilde{u} \qquad (32)$$

C_s may be obtained analytically. For 3D flow C_s =1, for 2D flow C_s =2/3. For 2D wall boundary flow C_s =1/12, for 3D wall boundary flow C_s=1/8 [2]. Equations (22), (25), and (31) plus two continuity equations

$$\nabla \cdot \overline{u} = 0 \qquad (33)$$

$$\nabla \cdot \widetilde{u} = 0 \qquad (33)$$

constitute the governing equations of incompressible turbulent flow. It is worthy to point out that these equations do not contain any empirical coefficients. Weighting coefficients M_1 and M_2 for the division of turbulence fluctuations into two groups are not explicitly appear, and thus need not to be determined.

7 Numerical examples

In order to verify the adaptability of the newly derived equations of incompressible turbulence, we compare computational results and experimental data for the following four benchmark flows. Both mean flow and intermittent coherent flow are calculated for each flow field. A standard SIMPLE scheme and staggered grid scheme are used for the finite difference formulations. A second order central difference form is used throughout the computation to avoid possible numerical error contamination. As a result, computational

stability relies on physical viscosity rather than artificial viscosity. All computations were performed on personal computers.

7.1 *Plan Jet*

Two-dimensional plane jet flow is a primary example to verify the spreading characteristic of typical free shearing flows. In the computation, the width of the jet nozzle is 2-cm wide and Re=3×10^4. The computation zone is a symmetric half domain, with length 1.0 m and width 0.3 m, divided by the jet central axis. The mesh size is 40×40 and the coefficient of substance C_s=2/3. Figure 1 shows the patterns of jet flow and its induced vortices obtained through the second-order energy equation (31) and smoothing scheme. The spreading rate is 0.105, which fell into the range of 0.10-0.11 measured in experiments [3].
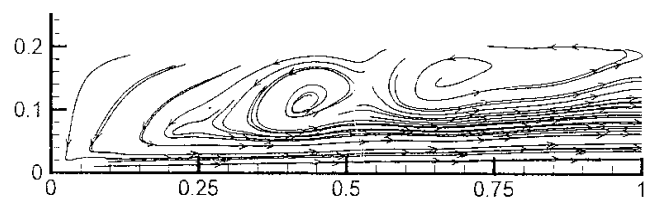
Figure 1. Flow pattern of plane jet. (n=2)
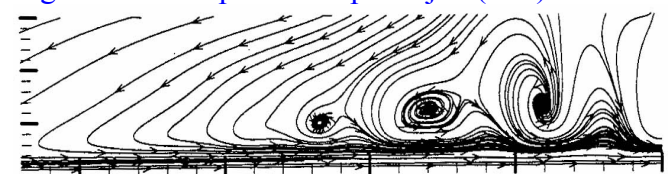
Figure2. Streamlines of coherent structures in plane jet.(n=1)

Figure 2 is one of the snaps of the computational results of first-order equation (31) without using the smooth scheme. The mesh size is 200×150. This set of results vividly displays the step by step formation process of entrainment vortices along the jet boundary. The intermittent coherent patterns are very similar to experimental photos [4].

7.2 Round Jet

Motivated by the plan/round jet anomaly, we simulated a round jet flow, $Re = 3\times10^4$. The computational symmetric half domain is 1-m

long and 0.2-m wide. A 41×61 mesh is used in the computational zone with uniform grid lengths in the direction of the central axis. Much denser grids are used near the central axis in the y direction to accommodate strong shear force and large velocity gradient. The coefficient of substance Cs=2(r-h)/3(r+h), where r is the radius of the center of the control volume, and h is the half width of control volume. The simulated results show that the spreading rate for the round jet is 0.086, which again falls in the range 0.086 ~0.093 measured from experiments [3]. The plane jet/round jet anomaly has been successfully eliminated. Figure 3 gives the comparison of velocity profiles in the y-direction at various locations. Self-preservation is clearly evident.
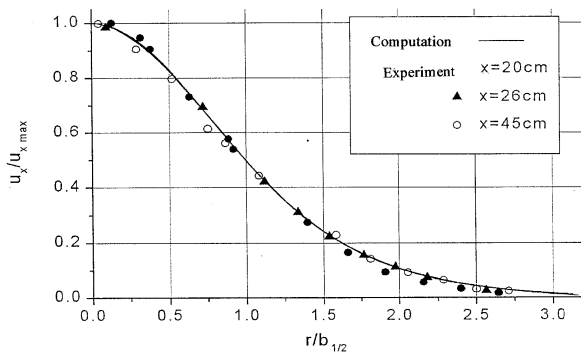
Figure 3. Self-preservation of velocity profile in round jet (n=2)

7.3 Boundary Layer and Transition on a flat-plate

The simulation of flat-plate boundary layer and transition is a real challenge to our newly developed equations of turbulence because they contain no empirical coefficients and no wall functions for possible adjustment.

Now, we consider a two-dimensional flow over a 6-meter long flat plate. The computational zone between the solid bottom and border of the top free flow is 3-meter wide. An 81×61 mesh is applied with an exponential distribution along the y-direction and a dense uniform distribution around the transition zone in the x-direction. The nearest 3-4 grids to the solid wall are within the laminar sublayer. Reynolds number is varying based on the length factor along the wall

direction. Within *10mm* thick near-wall region, the velocity at entrance has a laminar profile of *1/2* power, above which is a uniform velocity distribution with $Re=1.0×10^5$ at the entrance. The Reynolds number at the exit is $Re=2.2×10^7$. The coefficient of Substance C_s=1/12. Initial mean flow velocity is set to be 1 throughout the computation zone, while the initial drift flow is set to be zero. Shown in Figure 4 is the evolving process of the calculated mean velocity profiles and the thickness of the boundary layer around the transition zone by employing the second-order equation (31). The transition is shown around $Re=8×10^5$ area. To the authors' knowledge, all simulated details, such as the velocity profile, the thickness of boundary layer, friction coefficients, logarithmic velocity profile, form factor, and turbulence stresses, are in good agreement with experiments.
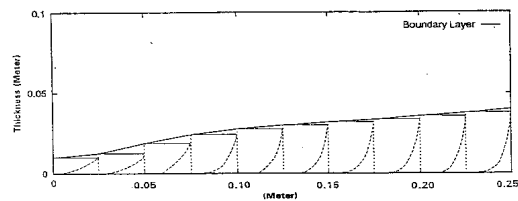
Figure 4. Velocity profiles in the transition zone of boundary layer (n=2)
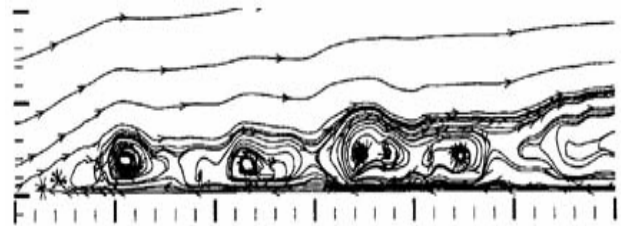
Figure 5. Intermittent patterns in boundary layer (n=1)

Figure 5 is a selected intermittent flow pattern of the boundary layer. In the computation, the same mesh, Reynolds number, and first order energy equation are adopted without using the smoothing scheme. Subtracting 0.8 U_e draws the intermittent patterns from the mean velocity at each grid point, where U_e is the free stream velocity. The two-dimensional results have clearly shown that the first-order energy equation (31) is the control equation for primary coherent structure.

The above results demonstrate that the present set of equations is able to calculate broad range of boundary layer flows from laminar to turbulent through transition.

7.4 Separation Flow over Backward Facing Step

The fourth example is a separation flow. According to case 0421 published in the 1980 Stanford Turbulence Conference [5], we calculated a flow over a backward-facing step. The computational zone is 20-m long and 4-m wide and $Re = 4.5 \times 10^4$. The step itself is 4-long and 2.5-m wide. A uniform mesh 100x60 covers the entire computational zone. Such mesh does not consider the effect of the boundary layer because the first grid near the wall is much thicker than the boundary layer. Such treatment may lead to larger friction on the non-slip boundary. However, it will not severely affect the shape of the recirculational vortex. When the first-order energy equation is used, the calculation demonstrates a complete process of vortex formation, growth, braking-up, and shedding. Figure 6 shows two snaps of the vortex shedding process.
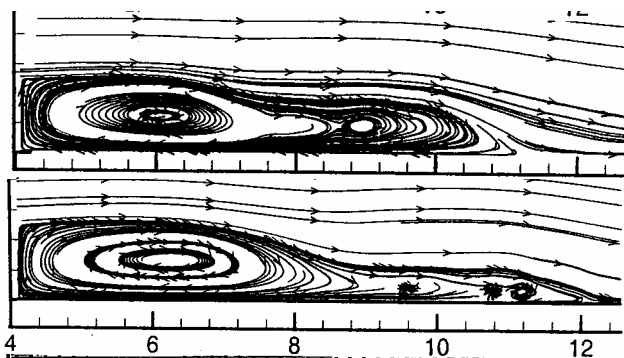
Figure 6. Vortex shedding behind a backward facing step (n=1)

When the third-order energy equation (31) is adopted, the vortex shedding and oscillation completely disappear and a steady vortex of length 6.9 is obtained (Figure 7), which falls in the experimental length data 6.5-7.5. The above results clearly show that the first-order energy equation dominates primary coherent structures and, therefore, constitutes a large eddy model,

and the higher-order equation constitutes a mean flow model.
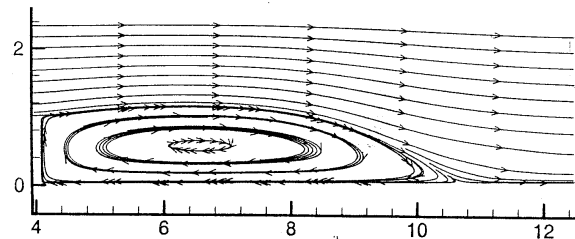
Figure 7. Mean flow pattern of backward-facing step flow obtained by higher-order energy equation.

8 Discussions

The objective of the present study is to present new equations of incompressible turbulence derived based on the physics of turbulence. These equations should be able to describe statistical mean flow and coherent flow simultaneously. As the Reynolds average completely loses the first-order statistical information of turbulence fluctuations, the second order information becomes the only tool to study the full influence of fluctuations upon the mean flow. Such a practice inevitably encounters many difficulties. Empirical coefficients have never been able to declare generality because they are lack of sound mathematical and physical bases. The research presented in this paper takes a very different path to study incompressible turbulence. The major methodology is as follows:

1. The introduction of the unilateral average scheme provides the first-order statistical information of the complex fluctuation field, based on which the useful momentum equation of drift flow and the independent mechanical energy equation are derived.

2. The symmetry of the weighted drift velocities puts a solid ground for introducing orthotropic coordinates, which greatly simplify the viscosity coefficient matrix and solve the problem of anisotropy. The symmetric property of the two weighted drift flows clearly demonstrates that the universal symmetric law found in

nature also exists in such a highly random event as turbulence.

3. The modeling of the correlation terms relies upon the phenomenological concept of the momentum transfer chain. The endless cascade down process of eddies and the decaying process of coherent structures from lower-order to higher-order are merely apparent disorder phenomena. Behind these phenomena, the authors believe that there is a deterministic momentum transfer chain starting from the mean flow to the drift flow, and eventually to random molecular motion. This modeling consists with physical reality of turbulence and eliminates the reliance on empirical coefficients.

4. The concept of orthotropy is popular in mechanics of composite materials. There is obvious similarity between wood grains and water grains. Introduction of the orthotropic concept into the modeling of turbulence viscosity greatly simplifies the matrix of viscosity coefficients through reducing 36 coefficients of three-dimensional non-isotropic matrix to 6. Multiplication of the drift velocity and the mean displacement length vector provides 9 tensor components, in which six shear stress coefficients compose three engineering shear stress coefficients plus three normal stress coefficients. When the coordinates deflect from the orthotropic coordinates, 36 non-zero coefficients appear again like a usual non-isotropic case. The eddy viscosity tensor and turbulence stresses obtained in this study are very different from the ones obtained based on the conventional isotropic eddy concept.

5. The independent mechanical energy equation (31) gives raise the relationship between the mean flow energy and the drift flow energy. It is known that the effect of the drift flow on the mean flow is to resist the mean flow motion. The work done by the drift flow over a displacement should be equal to the loss of the kinetic energy of the mean flow over the same displacement. This equation is unlike the conventional mechanical energy equation that is dependent on the momentum equation. The present mechanical energy equation is a bridge connecting the mean flow and the drift flow. The more series terms of the energy equation are used, the more accurate statistical mean solutions are possible.

6. The series form of the energy equation provides multiple discrete length-scales to describe infinite layers of turbulence structures and eddies. It is noticed that (31) is an algebraic equation for displacement vector. Its solution λ is discrete both in time and in space. So are the eddy viscosity tensor and turbulence stresses. In order to smooth turbulence mean stresses, we need to average the displacement vector at the end of computation. If the average were performed at each iteration step, the computation would give rise incorrect results. One of the examples is the simulated round jet flow, which failed to show the correct spreading rate. Apparently, the averaged solution of (31) is no longer the solution of the original nonlinear equation. This phenomenon deserves further investigation in view of philosophy and methodology in the study of nonlinear science.

The ability of simultaneously simulating mean flow and coherent flow of turbulence shows that newly developed turbulence equations have provided a hope to unite statistical and structure movements. Since the calculation of coherent flows can be performed on meshes of 10^3 to 10^5 grids, the original aim of large eddy simulation model is also realized. Of cause, for coherent structures, detailed study of three-dimensional calculations is needed.

9 Conclusion

The essential theme of the present approach is the application of the unilateral statistical average scheme to turbulent fluctuations. As the first step toward solving the closure problem, the first order statistical information is extracted from the fluctuations to characterize orthotropic turbulence and the momentum transfer train. It is assumed that the turbulence fluctuations constitute an orthotropic environment for the mean flow. The momentum transfer train is introduced based on the physics of the momentum transfer from mean flow to drift flow through viscosity and finally to molecular heat. These physical descriptions enables one to model correlation terms arising from the unilateral average and remove the need of empirical coefficients and wall functions in the equations of turbulence. The same set of equations is able to produce promising results in the numerical computation for quite different turbulent flow conditions, ranging from various mean flows to coherent flows.

The calculations of four kinds of benchmark turbulent flows, i.e. free shearing flows, boundary transition flow and separation flow, have proved that the same set of equations may provide precise statistical mean results as well as vivid coherent structure flows on sparse meshes. Since using the present equations has solved several difficult problems, such as transition, plane jet/round jet anomaly and vortex shedding phenomenon, the wide adaptability of the equations has obtained initial proof. It is promising that the set of equations may be used for further theoretical and engineering study of turbulence.

As turbulence is one of representative problems of nonlinear science, the methodology used in the present study of turbulence, such as unilateral average, the symmetry of the drift flows, orthotropic eddy viscosity, momentum transfer chain, the series form of independent mechanical energy equation and its discrete solution, may provide reference of mathematical-physical method for general nonlinear science.

References

[1] Gibson R. *Principles of Composite Material Mechanics*. 1st edition, Mc Graw-Hill press, 1994.

[2] Gao G and Yong Y. (2000). The United Modeling Theory for Both of Mean Flow and Coherent Flow of Incompressible Turbulence. *Journal of Aerospace Power* ,Vol.15, No.1,2000.

[3] Wilcox D. *Turbulence Modeling for CFD*. 1st edition, DCW Industries Inc, 1993.

[4] Lesieur M. *Turbulence in Fluids*. 2nd edition, Matinus Nijohoff Publishers,1987.

[5] *1980-1981 AFOSR-HTTM- Stanford Conference on Complex Turbulent Flows.*